

GRAPH-CUT METHOD FOR SEGMENTATION OF RETINAL VASCULAR NETWORK

SOUMYASHREE KODLIWAD¹, V. R. UDUPI² & SUBRAHMANYA K. N³

¹M. Tech Scholar, Departement of Electronics and Communication Engineering, GIT, Belgaum, India

²Professor, Departement of Electronics and Communication Engineering, GIT, Belgaum, India

³Assistant Professor, Departement of Electronics and Communication Engineering, GIT, Belgaum, India

ABSTRACT

Optical diagnosis could be efficient and reliable by the exact analysis of retinal structures. The paper presents an automated method for the segmentation of retinal blood vessels in retinal images. Algorithm begins with the enhancement of vessels by morphological operations, followed by extraction of retinal vascular network by the graph cut method. The proposed method could be used to assist the computer aided diagnosis in modern ophthalmology since the study of vascular network is of major interest while in diagnosis of retinal dsiseases like diabetic retinopathy, glaucoma and haemorrhages. The performance of suggested method in terms of accuracy, sensitivity, specificity and precision are tested and analysed on a publicly available DRIVE database.

KEYWORDS: DRIVE Database, Graph-Cut Method, Retinal Structure, Vessel Segmentation

INTRODUCTION

In modern ophthalmology, acquired retinal images are used for the detection and diagnosis of vascular disorders and maladies identified with an eye. Unfortunately, many patients remain undiagnosed as loss of vision is often a late symptom of advanced diabetic retinopathy. Periodic eye check-up for diabetic retinopathy screening can prevent the disease. The ophthalmologists acquire and use retinal images to assist in the analysis of anatomical structure. So that the results of analysis could be used to locate abnormalities in the eye structure and look for a change in lesions while diagnose of the disease.

Morphological features of retinal blood vessels like length, diameter and tortuosity have pertinence with the disease diagnose and can be used to predict the stages of diseases [1] such as glaucoma, diabetic retinopathy, vein occlusion and hypertension. But in some medical applications like detection of pathological elements like haemorrhages and neovascularization, the vascular structure must be excluded to facilitate the analysis and disease diagnosis [2]. Consequently there is a need for exact segmentation of blood vessels from retinal images.

Manual delineation could be employed by ophthalmologists for analysing morphological features of vascular network and shape of optic disc from retinal images. But this approach is unsubstantial and unfeasible. Because it is a highly skilled task and requires well instructed staff, unreliable when the morphology of vascular network is complex, tedious when number of images to be analyzed are huge, even susceptible to errors, time-consuming, and expensive. As a consequence there is a need for reliable automated system for the segmentation of vascular network and optic disc from retinal images such that vessel and optic disc characteristics are preserved for further analysis.

The automated segmentation method performs automatic segmentation of the vascular network and the optic disc.

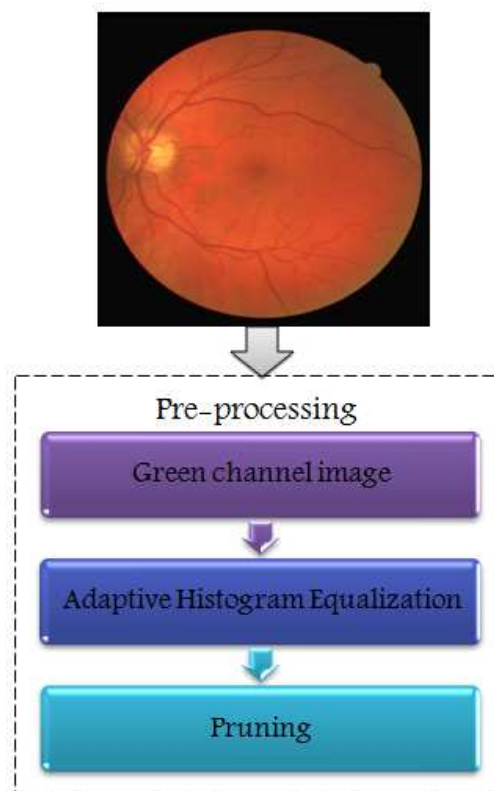
With this automation, ophthalmologists can examine features of retinal structures and efficiently perform mass screening exams for diagnosis as well as treatment of retinal diseases. This could prevent vision diminution, vascular disorders and cardiovascular diseases. The automated segmentation technique is a cost effective method, which could save time, and even reduces the stress of ophthalmologist. Therefore the automated system supports ophthalmologists to dissect huge dataset of retinal images in a methodical manner with the high precision within a short span.

Motivation

Numerous segmentation techniques have been reported in the literature for the delineation of retinal vascular network. But acquisition of retinal images under varying illuminations, resolution, angle of capture and tissue overlapping in retinal images lead to considerable degradation to the performance of automated segmentation of retinal structures. Hence there is always a room for improvement with respect to design of segmentation algorithm. Special consideration must be taken while choosing automated segmentation technique such that the corresponding technique provides precise segmentation results. As a consequence researches are being carried out to design robust algorithm for segmentation of retinal blood vessels.

Objective

In the proposed method, automated technique is presented for the delineation of retinal structure such as vessel networks from retinal images. The overall segmentation system of retinal structures is shown in Figure 1. In the first stage, retinal images of database are pre-processed to obtain enhanced binary image. Later vascular network is segmented from retinal images by employing graph-cut technique. The performance metrics of proposed method are examined in terms of accuracy, sensitivity, specificity and precision on publicly available DRIVE database.



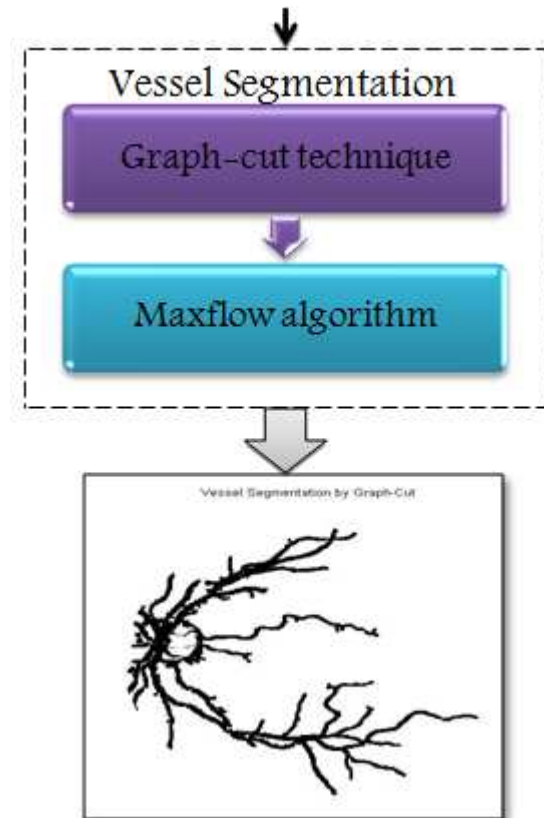


Figure 1: Segmentation System of Retinal Vasculature

Literature survey

There are two main approaches considered for retinal vasculature segmentation: Pixel processing based techniques and Tracking based techniques. The performance metrics of the following surveyed papers on publicly available STARE and DRIVE datasets are tabulated in Table 1.

Pixel Processing Based Methods

Pixel processing based methods are two-stage approaches. The principal stage involves a mechanism of enhancement, where filters are used to intensify the aspect of blood vessels in the retinal images. The second step is validation of vessel pixels, where thinning or branching techniques are applied to characterize the pixel as either vessel or non-vessel. This type of approach processes each and every pixel of an image to resolve whether the comparing pixel fits in with blood vessels.

Chaudhuri et al. in [3] presented the concept of matched filter for the recognition of blood vessels as ‘segments’. Twelve different kernels and templates were employed to look for all vessel segments along all the conceivable orientations. Validation of segments was based on thresholding. This method retains computational simplicity because of employing thresholding based edge operations. But the system takes long time for execution because of large kernel size. *Hoover et al.* in [4] employed a set of twelve directional kernels and then applied piecewise threshold-probing technique for vessel segmentation. This method reduces false positives by 15 times than conventional thresholding of MFR. But connectedness property isn’t captured, so it fails to validate vessels in small group in the form of isolated pixels in retinal images. *Staal et al.* in [5] proposed a supervised technique called ridge-based or primitive-based technique for vessel

segmentation. This method is in view of the property that the vessels are prolonged structures. It results into missing or erroneous vessel branch detection mostly while detecting small vessels and over or under vessel segmentation which would affect the performance of systems while determining width of vessels. *Mendonca et al.* in [6] presented a framework to extract blood vessels by detecting vessel centrelines. Algorithm was mainly divided into three steps: Pre-processing phase, Vessel centerline detection phase, and Vessel segmentation phase. But it results into under segmentation for few vessel segments due to intensity variation in the vessel regions. *B. Zhang et al.* in [7] proposed a method by combining First Order Derivative of Gaussian with Matched Filter (MF-FODG). Retinal image response to Matched Filter (MF) was thresholded to detect the vessels, while threshold was tuned by image response to First Order Derivative Gaussian (FODG). This method reduces false detections caused from Matched Filter (MF) and detects many fine vessels.

Tracking Based Methods

Tracking or Tracing based methods use a single stage approach. It starts by locating the vessel points for tracing the vascular network, by assessing image properties. The image feature's extraction and the recognition of vasculature are simultaneously performed. Localization of the initial vessel point can be manual or automatic. In the manual tracing, the user selects the initial vessel point and they generally provide accurate vessel segmentation. In the automatic tracing, the initial vessel point is automatically selected by algorithm, which utilizes a Gaussian function to characterise a vessel profile model to head forward and segment a vessel, which are computationally efficient and more preferable for retinal image processing.

Zhou et al. in [8] presented an algorithm based on matched filter approach paired with the prior information about properties of blood vessels. This method detects vessel boundaries automatically, track centreline of vessel and thus segment blood vessels. This method provides improvement on accuracy of diameter measurement of vessels due to Gaussian fittings. But it results into Missing of the vessels that underlay or overlay on the main vessel which are almost perpendicular to each other. *Martinez-Perez et al.* in [9] proposed a technique based on second directional derivative of image intensity. The features obtained at multiple levels derived from image derivatives were employed in two stage region growing procedure for progressive segmentation of the blood vessels. This method overcomes the intensity variations in retinal images while segmentation. *Xu et al.* in [10] presented a method combining the tracking growth technique and the adaptive local thresholding method for retinal blood vessel segmentation. This method employed local thresholding and extracted large connected components as vessels. Tracking growth technique was then applied to thin vessels to frame entire vascular network. This method overcomes the variations in contrast between large and thin vessels.

Table 1: Performance Metrics of Vessel Segmentation Methods

Methods	STARE Dataset		DRIVE Dataset	
	Accuracy	TPR	Accuracy	TPR
Chaudhuri et al.	0.9384	0.6134	-	-
Hoover et al.	0.9267	0.6751	-	-
Staal et al.	0.9541	0.6970	0.9442	0.7194
Mendonca et al.	0.9440	0.6996	0.9452	0.7344
Zhang et al.	0.9484	0.7177	0.9382	0.7120
Martinez-Perez et al.	0.9181	-	-	-

BLOOD VESSEL SEGMENTATION

Segmentation of blood vessels involves two steps: Pre-processing and Graph-cut technique. Blood vessel

segmentation algorithm is initialized by Pre-processing, which consists of Adaptive Histogram Equalization (AHE) and pruning followed by Graph-cut method. It is illustrated in the Figure. 2.

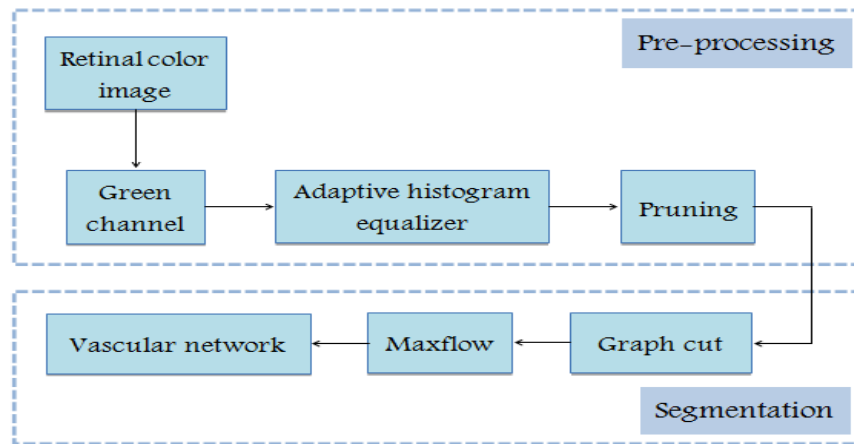


Figure 2: Block Diagram of Vessel Segmentation

Pre-Processing

Initially the green component image is extracted from the retinal colour image which generates intensity inverted image as shown in the Figure 3 (d). Then the Contrast enhancement adaptive histogram equalizer is applied to the resultant image followed by the pruning process as shown in the Figure 2.

Adaptive Histogram Equalization (AHE)

Image enhancement is performed by an adaptive histogram equaliser equation which is given by:

$$I_{\text{Enhanced}} = \left(\sum_{p' \in R(p)} \frac{s(I(p) - I(p'))}{h^2} \right)^r \cdot M \tag{1}$$

Where h denotes Window or Block size, r denotes Controls the level of enhancement, M is Maximum intensity value in the image (255), and $p' \in R(p)$ is the Square window of the length h. I denotes Green component of retinal colour image, p is a Pixel, p' is neighborhood pixels around p with $(I(p) - I(p')) = d$,

Where,

$$s(d) = \begin{cases} 1, & d > 0 \\ 0, & \text{else} \end{cases} \tag{2}$$

Initially the image to be enhanced is divided into blocks with the block size of 'h'. Experimentally, the value of block size (h) is found to be 5. Hence number of blocks in an image of size (m X n) is (m/h + n/h) neglecting the fractional part. For example, image of size (580 X 560) consists of (580/5 + 560/5) = 228 blocks. Centre pixel I(p) of a block is subtracted with neighborhood pixels I(p'). Then the value of s(d) is decided based on 'd' as per equation 2. Arithmetic operations are applied further as per the equation 1, such that intensity level of each block of an image is inverted. These steps are repeated for every block of an image so that the image is enhanced as shown in the Figure 3.3. The parameter 'r' controls the level of enhancement such that the contrast between vessel pixels and background is increased by increasing the value of 'r'.

Pruning

As shown in the Figure 2, binary morphological operations or filters are applied to prune the enhanced image, which eliminates all the misclassified pixels. This technique effectively reduces the false positives and aids to enhance the performance of segmentation as shown in the Figure 3. The resulting pruned image will be used for construction of the graph, which is a major step of vessel segmentation. Figure 3 (b), (c), (e), (f) shows the resulted enhanced and pruned images with varying values of 'h', 'r'. From the observation, it can be interpreted that the performance of segmentation increases with the increase in values of window size h and r.

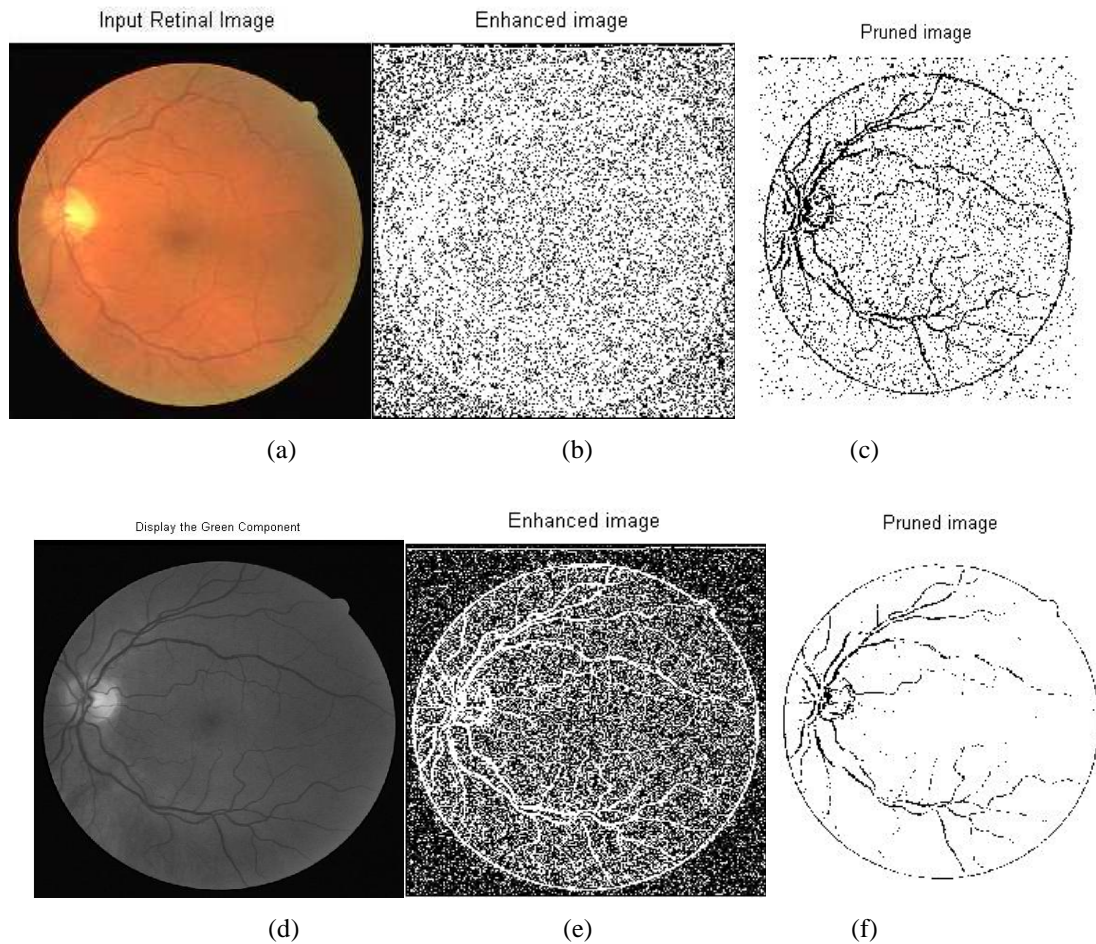


Figure 3: (a) Retinal Colour Image, (b) Enhanced Image with $h=3$, $r=6$, (c) Pruned Image with $h=3$, $r=6$, (d) Green Channel Image of Retinal Colour Image, (e) Enhanced Image with $h=5$, $r=6$ (f) Pruned Image with $h=5$, $r=6$

Graph-Cut Technique

Graph-cut technique has wide range of application in segmentation of an object from the image. This technique is characterised by an optimisation operation intended to minimize the energy generated from a given image. This energy defines the correlation between neighbourhood pixel components in an image. Graph-cut technique is employed in proposed retinal structure segmentation, similar to the work presented in [18]. Segmentation by graph-cut technique can be illustrated as shown in the Figure 4.

A graph $G(N, E)$ is defined as a set of nodes (pixels) 'N' and a set of undirected edges 'E', where the edges unite

neighbouring nodes. The graph incorporates two unique nodes: a foreground terminal (Source ‘S’) and a background terminal (Sink ‘T’), where source refers to vessel pixels. It can be illustrated by the Figure 4 (a).

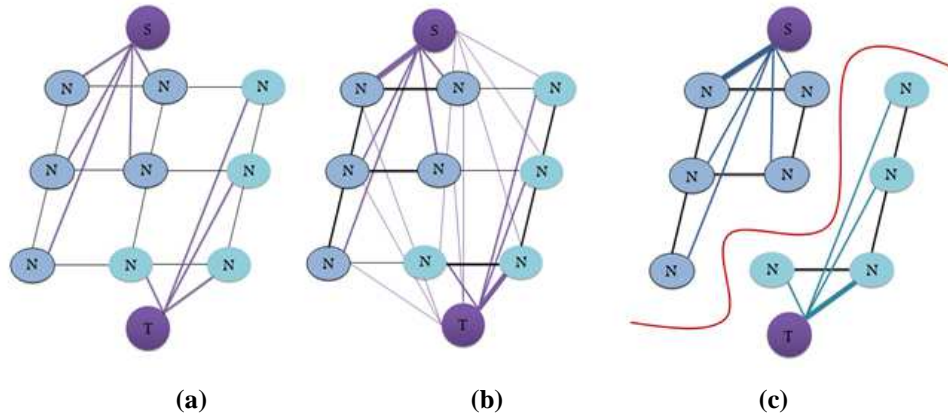


Figure 4: (a) Image Pixel Connection with Special Nodes, (b) Weight Assignments for Edges, (c) Graph-Cut Segmentation

An undirected edge ‘E’ incorporates two types of undirected edges: neighbourhood links (n-links) and terminal links (t-links), where n-links connect neighbourhood pixels of an image and t-links connect image pixels to special nodes (either S or T). Every pixel $p \in P$ (a set of pixels) in the graph contains two t-links: $\{p, S\}$ and $\{p, T\}$ connecting pixel to each of the terminal, while a couple of neighbouring pixels $\{p, q\} \in N$ (number of pixel neighbour) is connected by n-links. Hence:

$$E = N \cup_{p \in P} \{ \{p, S\}, \{p, T\} \}, V = P \cup \{S, T\} \tag{3}$$

An edge $e \in E$ is assigned a weight (cost) of $W_e > 0$. A cut is defined by a subset of edges $C \in E$, where $G(c) = (N, E/C)$ is isolating the graph into foreground and background with ‘C’ defined as: $|C| = \sum_{e \in C} W_e$. Severed n-links are located at the segmentation boundary. Thus, their aggregate cost represents the cost of segmentation boundary. On the other hand, severed t-links represents the regional properties of segments. Consequently, a minimum cost cut results into the segmentation with a desirable balance between regional and boundary properties. Table 1 assigns weight to the edges E in the graph [19].

Table 2: Weight Assignments for Edges in the Graph

Edge	Weight	For
$\{ p, q \}$	$B_{\{p,q\}}$	$\{ p, q \} \in N$
$\{ p, S \}$ (foreground)	$\lambda \cdot R_p(F_g)$ K 0	$p \in P, p \in F \cup B$ $P \in F$ $P \in B$
$\{ p, T \}$ (background)	$\lambda \cdot R_p(B_g)$ K 0	$p \in P, p \in F \cup B$ $P \in F$ $P \in B$

Where,
$$K = 1 + (\max_{p \in P} \sum_{\{p,q\}} B_{p,q}) \tag{4}$$

‘F’ and ‘B’ represent the subset of pixels selected as foreground and background respectively. Therefore $F \subset P$ and $B \subset P$ such that $F \cap B = \emptyset$. $B_{p,q}$ defines the discontinuity between neighbouring pixels. $\lambda > 0$ is a constant

coefficient, which is defined in the energy formulation graph. Weight assignments are carried out for an image as shown in the Figure 4 (b), where the link thickness is represented unequally to depict their respective weights.

The Graph-cut technique is employed in the proposed segmentation since “it allows the incorporation of prior knowledge into the graph formulation to guide the model and hence find the optimal segmentation.” Let $A = (A_1, \dots, A_p, \dots, A_p)$ be binary set of labels assigned to each pixel ‘p’ in an image, where A_p signifies assignments to the pixel ‘p’ in ‘P’. Subsequently, each assignment A_p is either in Foreground (F_g) or in Background (B_g). Accordingly the segmentation is obtained by the binary vector ‘A’ and the constraints imposed on the regional and boundary properties of vector ‘A’ are derived by an energy formulation of the graph, which can be defined as:

$$E(A) = \lambda \cdot R(A) + B(A) \quad (5)$$

Where the positive coefficient ‘ λ ’ denotes the relative importance of regional term (likelihoods of foreground and background) ‘ R_A ’ over the boundary term (relationship between neighbourhood pixels) ‘ B_A ’. the regional term or the likelihood of the foreground and background term is given by:

$$R(A) = \sum_{p \in P} R_p(A_p) \quad (6)$$

The regional term $R(A)$ assumes the special penalty for assigning pixel ‘p’ to the foreground and background, which can be denoted as $R_p(F_g)$ and $R_p(B_g)$ respectively. $R_p(A_p)$ specifies the assignment of pixel ‘p’ to either the Foreground (F_g) or Background (B_g). For instance, how the intensity of pixel ‘p’ fits into the given intensity models (Ex: Histograms) of the object and background may be intervened by $R_p(*)$, given by the equations 7 and 8 and the boundary constraints [16] is defined by equation 9 as follows:

$$R_p(F_g) = -\ln \Pr(I_p | \text{"obj"}) \quad (7)$$

$$R_p(B_g) = -\ln \Pr(I_p | \text{"bkg"}) \quad (8)$$

$$B(A) = \sum_{p,q \in N} B_{p,q} \cdot \phi(A_p, A_q) \quad (9)$$

$$\text{Where,} \quad \phi(A_p, A_q) = \begin{cases} 1, & A_p \neq A_q \\ 0, & \text{else} \end{cases} \quad (10)$$

$$B_{p,q} = \exp\left(-\frac{(I_p - I_q)^2}{2\sigma^2}\right) \cdot \frac{1}{\text{dist}(p,q)} \quad (11)$$

This function penalizes a lot for discontinuities between pixels of similar intensities when $|I_p - I_q| < \sigma$. But if pixels are altogether different when $|I_p - I_q| > \sigma$, then penalty is small. $B_{p,q}$ defines the discontinuity between neighboring pixels. Its value is large when the pixel intensities (I_p and I_q) are similar and its value is close to zero when they are different. The distance $\text{dist}(p, q)$ between the pixels ‘p’ and ‘q’ also affects the value of $B_{p,q}$.

Maxflow Algorithm

Maximum flow algorithm routes the flow as much as possible from source (S) to the sink (T) to compute minimum S-T cuts on the graph. It gradually increases the flow from source (S) to sink (T) along the edges until enough edges are found for the boundary (cut) to segregate the terminals. At the end of algorithm, Maximum Flow saturates the graph and the edges thus found are said to be saturated edges which corresponds to Minimum Cut on the graph resulting in

optimal segmentation as shown in the Figure 4 (c). After employing this Maxflow algorithm for the graph of an image, vascular network is segmented from the background as shown in the Figure 5.

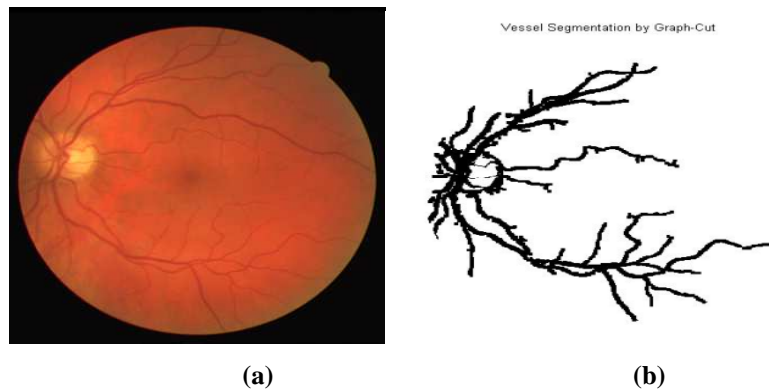


Figure 5: (a) Retinal Colour Image, (b) Segmented Blood Vessels of Retinal Image

RESULTS AND DISCUSSIONS

It is denoted that True Positives (TP) and True Negatives (TN) represents the properly identified vessel pixels and background pixels respectively. False Positives (FP) illustrates the background pixels which are mistakenly recognized as vessel pixels and False Negatives (FN) represents the pixels belonging to a vessel, however erroneously perceived as background pixels. Table 5.2 lists the results of vessel segmentation performed on the DRIVE dataset in MATLAB environment. The performance measures can be defined and calculated as follows:

- **Accuracy:** The accuracy represents the fraction of correctly recognized pixels from the image field of perspective while the detection of vessels.

$$\text{Accuracy} = \frac{TP+TN}{TP+FP+TN+FN} * 100 \quad (12)$$

- **True Positive Rate (TPR) or Sensitivity:** The True Positive Rate (TPR) represents the fraction of pixels correctly identified as vessel pixels.

$$\text{TPR} = \text{Sensitivity} = \frac{TP}{TP+FN} * 100 \quad (13)$$

- **False Positive Rate (FPR):** The False Positive Rate (FPR) represents the fraction of pixels erroneously identified as vessel pixels.

$$\text{FPR} = \frac{FP}{FP+TN} * 100 \quad (14)$$

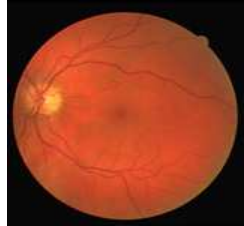
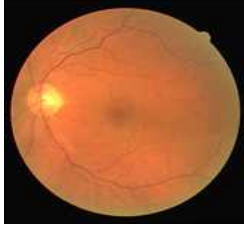
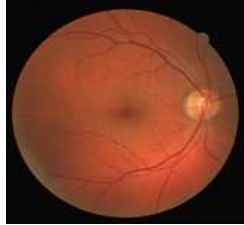
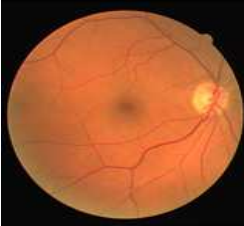
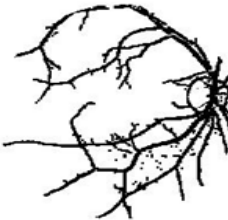
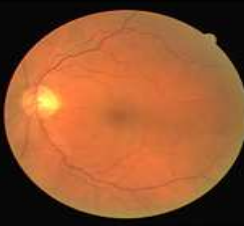
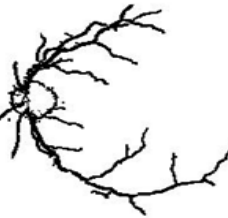
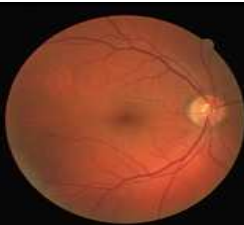
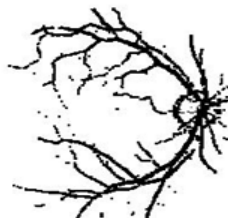
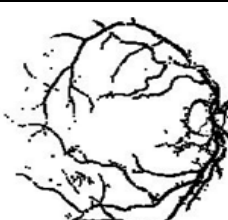
- **Precision:** The precision represents the correctness of properly identified vessel pixels out of properly identified pixels in the image field of perspective.

$$\text{Precision} = \frac{TP}{TP+FP} * 100 \quad (15)$$

- **Specificity:** The specificity represents the fraction of pixels correctly identified as background pixels. It can also be represented in terms of FPR as:

$$\text{Specificity} = 1 - \text{FPR} = \frac{TN}{TN+FP} * 100 \quad (16)$$

Table 4: Vessel Segmentation Results

no	Retinal images	Vessel segmented images	Performance metrics (%)	
1			Accuracy	92.3923
			TPR	50
			FPR	3.7476
			Precision	54.8504
			Specificity	96.2524
2			Accuracy	89.8569
			TPR	50
			FPR	8.6798
			Precision	17.4566
			Specificity	91.3202
3			Accuracy	90.6358
			TPR	50
			FPR	8.4725
			Precision	11.4647
			Specificity	91.5275
4			Accuracy	91.2441
			TPR	50
			FPR	7.2061
			Precision	20.6805
			Specificity	92.7939
5			Accuracy	91.7540
			TPR	50
			FPR	4.9074
			Precision	44.8936
			Specificity	95.0926
6			Accuracy	91.6224
			TPR	50
			FPR	3.5316
			Precision	62.2404
			Specificity	96.4684
7			Accuracy	91.8224
			TPR	50
			FPR	3.0322
			Precision	66.9828
			Specificity	96.9678

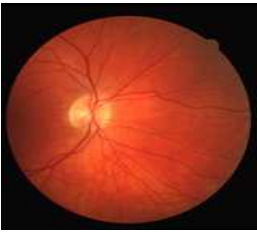
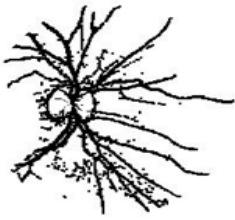
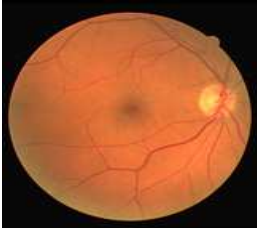
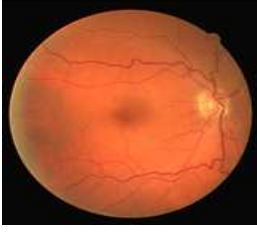
no	Retinal images	Vessel segmented images	Performance metrics (%)	
8			Accuracy	92.7150
			TPR	50
			FPR	2.9192
			Precision	63.6444
			Specificity	97.0808
9			Accuracy	90.8117
			TPR	50
			FPR	4.1233
			Precision	60.0785
			Specificity	95.8767
10			Accuracy	90.8037
			TPR	50
			FPR	4.0109
			Precision	61.3036
			Specificity	95.9891

Table 4 lists few of the standard retinal images of the DRIVE database, vessel segmented images, performance measures: Accuracy, True Positive Rate (TPR), False Positive Rate (FPR), Precision and Specificity. Performance metrics are computed as mentioned previously in the same section.

Average or mean value of Performance metrics calculated for 40 images of DRIVE database are as follows, which are plotted in the Figure 6 :

- Mean accuracy = 91.1533 %
- Mean TPR = 50 %
- Mean FPR = 5.1844 %
- Mean Precision = 46.079 %
- Mean Specificity = 94.7361 %

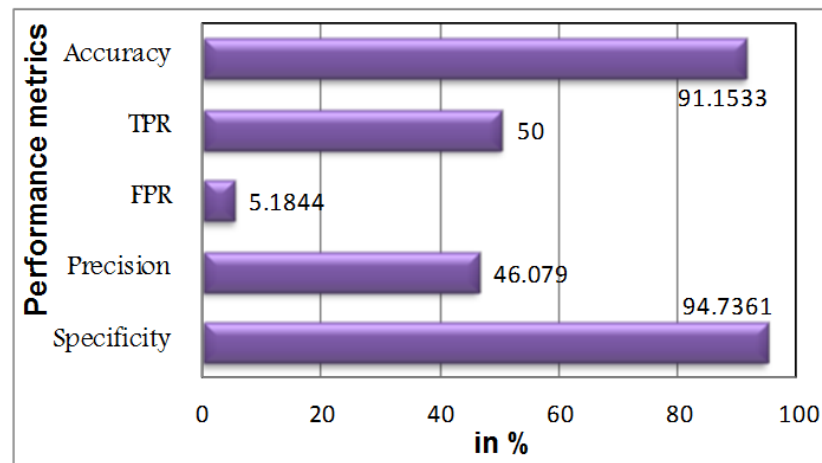


Figure 6: Performance Metrics of Vessel Segmentation

CONCLUSIONS

Robustness of the segmentation process is crucial to accomplish more precise and proficient computer aided diagnostic system in ophthalmology. Proposed system exhibits an automated algorithm for segmentation of retinal blood vessels. It is not expected that the automated frameworks will supplant the human experts in diagnosis; rather they will reduce stress and workload of the experts in examining the large number of retinal images. This could save time and assist ophthalmologist to analyze huge database of retinal images in a systematic manner with the high accuracy within a short span. Although many promising segmentation techniques have been reported, it is still an open area for research with the aim of replacing human experts.

REFERENCES

1. M. E. Martinez-Perez, A. D. Hughes, A. V. Stanton, S. A. Thom, N. Chapman, A. B. Bharath, and K. H. Parker, "Retinal vascular tree topology: A semi-automatic quantification," *IEEE Trans. Biomed. Eng.*, Vol. 49, No. 8, PP. 912-917, Aug. 2002.
2. M. Niemeijer, B. Van Ginneken, J. J. Staal, M. S. A. Suttorp-Schuilten, and M.D. Abramoff, "Automatic detection of red lesions in digital color fundus photographs," *IEEE Trans. Med. Imag.*, Vol. 24, No. 5, PP. 584-592, May 2005
3. S. Chaudhuri, S. Chatterjee, N. Katz, M. Nelson, and M. Goldbaum, "Detection of blood vessels in retinal images using two-dimensional matched filters," *IEEE Trans. Med. Imag.*, Vol. 8, No. 3, PP. 263-269, 1989.
4. A. Hoover, V. Kouznetsova, M. Goldbaum, "Locating blood vessels in retinal images by piecewise threshold probing of a matched filter response," *IEEE Trans. Med. Imag.*, Vol. 19, No. 3, PP. 203-210, 2000.
5. J. Staal, M. D. Abramoff, M. Niemeijer, M. A. Viergever, and B. Van Ginnekan, "Ridge-based vessel segmentation in color images of the retina," *IEEE Trans. Med. Imag.*, Vol. 23, No. 4, PP. 501-509, Apr. 2004.
6. A. M. Mendonca, and A. Campilho, "Segmentation of retinal blood vessels by combining the detection of centerlines and morphological reconstruction," *IEEE Trans. Med. Imag.*, Vol. 25, No. 9, PP. 1200-1213, 2006.
7. A. Zhang, L. Zhang, L. Zhang, and F. Karray, "Retinal vessel extraction by matched filter with first order

- derivatives of Gaussian,” *Computers in Bio. and Med.*, Vol. 40, No. 4, PP. 438-445, 2010.
8. L. Zhou, M. S. Rzeszutarski, L. J. Singerman, and J. M. Chokreff, “The detection and quantification of retinopathy using digital angiograms,” *IEEE Trans. Med. Imag.*, Vol. 13, No. 4, PP. 619-626, 1994.
 9. M. E. Martinez-Perez, A. D. Hughes, A. V. Stanton, S. A. Thom, A. A. Bharath, and K. H. Parker, “Segmentation of retinal blood vessels based on the second directional derivative and region growing,” *ICIP Proc.*, PP. 173-176, 1999.
 10. L. Xu, and S. Luo, “A novel method for blood vessel detection from retinal images,” *Biomed. Eng. Online*, Vol. 9, No. 1, PP. 14, 2010.
 11. A. Aquino, M. E. Gegundez-Arias, and D. Marin, “Detecting the optic disc boundary in digital images using morphological, edge detection, and feature extraction techniques,” *IEEE Trans. Med. Imag.*, Vol. 29, No. 11, PP. 1860-1869, 2010.
 12. H. Yu, E. S. Barriga, C. Agurto, S. Echegaray, M. S. Pattichis, W. Bauman, and P. Soliz, “Fast localization and segmentation of optic disk in retinal images using directional matched filtering and level sets,” *IEEE Trans. Info. Tech. Biomed.*, Vol. 16, No. 4, PP. 644-657, 2012.
 13. M. D. Saleh, N. D. Salih, C. Eswaran, and J. Abdullah, “Automated segmentation of optic disc in fundus images,” *IEEE 10th International Colloquium Signal Proc. and its applications*, PP. 145-150, 2014.
 14. J. Lowell, A. Hunter, D. Steel, A. Basu, R. Ryder, E. Fletcher, and L. Kennedy, “Optic nerve head segmentation,” *IEEE Trans. Med. Imag.*, Vol. 23, PP. 256-264, Feb. 2004.
 15. R. Chrastek, M. Wolf, K. Donath, H. Niemann, D. Paulus, T. Hothorn, B. Lausen, R. Lammer, C. Y. Mardin, and G. Michelson, “Automated segmentation of the optic nerve head for diagnosis of glaucoma,” *Med. Imag. Analysis*, Vol. 9, No. 1, PP. 297-314, 2005.
 16. D. Welfer, J. Scharcanski, C. Kitamura, M. D. Pizzol, L. Ludwig, and D. Marinho, “Segmentation of the optic disc in color eye fundus images using an adaptive morphological approach,” *Computers in Bio. and Med.*, Vol. 40, No. 1, PP. 124-137, 2010.
 17. Jun Cheng, Jiang Liu, Yanwu Xu, Fengshou Yin, D. W. K. Wong, Beng-Hai Lee, C. Cheung, Tin Aung, and Tien Yin Wong, “Superpixel classification for initialization in model based optic disc segmentation,” *IEEE Int. Conf. Eng. Med. Bio. Soc.-EMBC’2012*, PP. 1450-1453, 2012.
 18. Ana Salazar-Gonzalez, Djibril Kaba, Yongmin Li, and Xiaohui Liu, “Segmentation of blood vessels and optic disc in retinal images”, *IEEE Journal of Biomed. And Health Informatics*, Vol. 18, No. 6, PP. 1874-1886, 2014.
 19. Y. Y. Boykov, and M. P. Jolly, “Interactive graph cuts for optimal boundary & region segmentation of objects in N-D images,” *Proceedings 8th IEEE Int. Conf. – ICCV’2001*, Vol.1, PP. 105-112, 2001.
 20. A. Efros, and T. Leung, “Texture synthesis by non-parametric sampling,” *Proceedings ICCV’1999*, PP. 1033-1038, 1999.

